

# Detection of sub-cellular changes by use of $\lambda=6.5 \mu\text{m}$ laser light interaction in association with Intelligent Laser Speckle Classification (ILSC) technique

Ahmet Orun<sup>1</sup>

<sup>1</sup>De Montfort University, Faculty of Computing, Engineering and media, Leicester UK  
Email: aorun@dmu.ac.uk. Phone: +44(0)116 3664408

## Abstract

The study is based on a principle of laser physics so that a (coherent) laser light whose wavelength is shorter than a feature under inspection (like sub-cellular component) can interact with such specific feature (or textural features) and generates laser speckle patterns which can characterize those specific features. By the method we have managed to detect differences at sub-cellular scales such as genetic modification, cellular shape deformation, etc. with 87% accuracy. In this study red laser is used whose wavelength ( $6.5\mu\text{m}$ ) is shorter than a plant cell ( $\sim 60 \mu\text{m}$ ) that is suitable to interact with sub-cellular features. The work is assumed to be an initial stage of further application on human cellular changes observation that would be utilized for development of more accurate methods such as better drug delivery assessments, systemic diseases early diagnosis, etc.

## 1 Introduction

The laser speckle imaging application is well established method that has been already used for decades (almost since laser was invented) in the areas of industrial inspection, medical applications, material science, etc. The imaging method is based on physical phenomenon so that when a rough surface is illuminated by coherent light like laser, then the light scatters from the surface exhibits a particular intensity distribution covering the surface with fine granular form. In earlier studies photographic materials were used for laser speckle image formation. With the production of digital cameras the technique has become more advanced with digital recording facilities (for dynamic form of laser speckle analysis) at higher resolution and pixel based statistics. By exploiting the digital imaging facilities, the method was later unified with different texture analysis and learning classifiers (e.g. Bayesian, etc.) which is called "Intelligent Laser Speckle Classification (*ILSC*)" that was first introduced for material surface inspection in 2003 [8] and then for medical skin analysis work [1] and for medical tablet characterisation [11]. One of the most similar technique introduced by the earlier study [12] called *Laser speckle contrast imaging* which is based on moving features (e.g. blood circulation in micro-veins) as is not suitable for the observations of still cellular features. The method also relies on manual image analysis by naked eye without any use of AI method like *ILSC*.

The novel method called Intelligent laser speckle classification has potential applications for non-invasive human cells observations in real-time. The method can be used for systemic (skin related) diseases' early diagnosis, and can also be further applied to drug delivery assessment in pharmaceutical fields whenever human tissue is observable instead of plant's one. Such further test results would be justified if the expected cellular or sub-cellular changes would be detected that caused by the drug taken. On physical basis, the study is based on a principle of laser physics so that a (coherent) laser light whose wavelength is shorter than features to be inspected (like sub-cellular component) can interact with those features and generates laser speckle patterns that characterize those specific features under inspection. By the method we believe that, it would be possible to detect dynamic changes at sub-cellular scales such as genetic modification, cellular or cell nucleus shape deformation, etc. These conclusions have been made after the *ILSC* experiments in which healthy and diseased leaf tissues (Figure 1) were discriminated with 87% accuracy even though those two classes of tissues looked very identical to each other under the microscope magnification (Figure 3). In this study red laser is used whose wavelength ( $6.5\mu\text{m}$ ) is shorter than a plant cell ( $\sim 60 \mu\text{m}$ ) that is suitable to interact with sub-cellular features.

By the technique called Laser Speckle Imaging, the speckle images are acquired by a CCD camera and sampled from the image locations where laser-leaf tissue interaction is effective (generating characteristic patterns) as seen in Figure 2. In Figure 2, the diseased and healthy leaf tissues at the images of  $\lambda=6.5 \mu\text{m}$  laser Speckle sampling in  $200 \times 200$  pixel windows (refers to  $0.56\text{mm}^2$  each) with an image resolution of  $2.8 \mu\text{m}/\text{pixel}$ . The pattern differences between the diseased and healthy tissues are invisible to naked eye as is also in the microscope images in Figure 3.

## 2 Laser speckle phenomenon

According to the basic principle of “laser light-surface” interaction, when a rough surface is illuminated by a coherent light like laser then the light itself scatters from the surface exhibiting a particular intensity distribution as it looks covering the surface with a granular structure. The very fundamental formula of laser speckle image includes its pixel intensity statistics, where the standard deviation of spatial intensity variations  $\sigma_s$  is equal to the mean intensity  $\langle I \rangle$  for full developed (ideal) speckle pattern. This would be stated by the basic formula ;

$$K = \sigma_s / \langle I \rangle$$

Where  $K$  is the speckle contrast and its value takes place between 0 and 1. If the speckle pattern is ideal then  $K=1$ . But if the speckle pattern becomes not ideal such as blurred by a diffuser or surface motion, then value of  $K$  will be shifted towards zero.

## 3 Methods and Materials

### 3.1 Intelligent laser speckle classification

Within this work, the novel method called Intelligent Laser Speckle Classifier (ILSC) [11] is used having been tested also in earlier studies and yielding promising results [1][2][3]. The method consists of different components such as laser speckle imaging technique [4], texture analysis [5] and Bayesian classifier [6] that are merged to provide optimum classification of laser speckle patterns each specific to different class of tissues (diseased or healthy leaf tissues). For texture based quantization process of the LSIs, five statistical measures are used (derived from Phillips) [5]. Each texture's statistical characteristic is applied onto two different sizes of operation windows ( $3 \times 3$ ) which correspond to Equation. 1–4 and single measure at only  $3 \times 3$  window size corresponds to Equation 5. Each textural measure has been applied on two  $200 \times 200$  pixel areas on each LSI. As far as such texture analysis is concerned, large window size produce large edge effect at the class edges but provide more stable texture measures than small windows. In return, small window size is less stable but has smaller edge effect [7]. The texture measures used are shown by Formulas 1–5.

These texture measures had been previously tested on different material surface types in the experiments and yielded satisfactory results for surface texture analysis and surface type identification. The texture values of different classes (diseased and healthy leaf tissues) have then be analysed by Bayesian classifier to differentiate the subtle microscopic characteristic patterns which are invisible to eye under microscope magnification (Figure 3) and also even in laser speckle images (Figure 2)

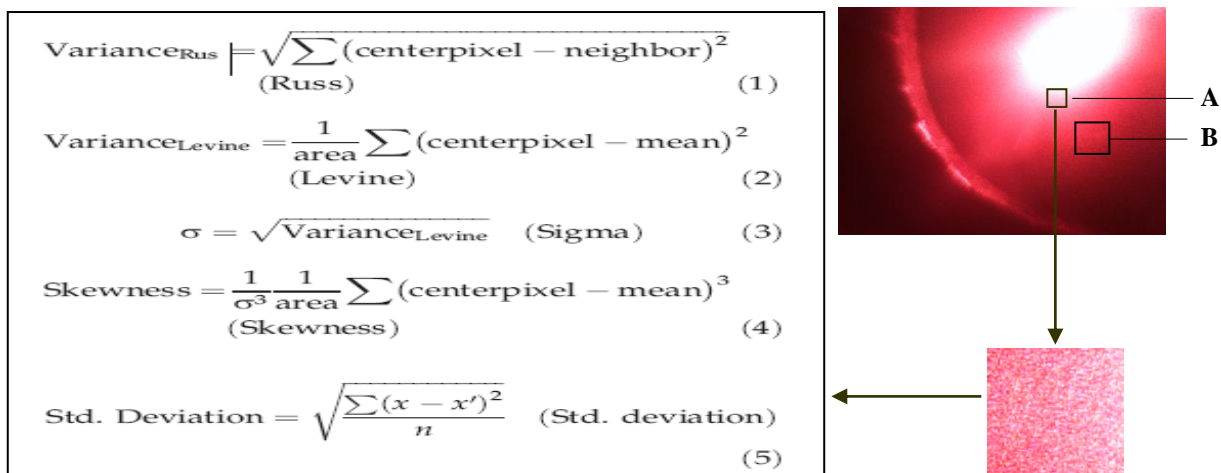


Figure 1a. Texture measures applied onto texture samples taken on the laser speckle image segments where There is high interaction between the laser light and leaf tissue cellular features (for diseased and healthy leaves)

### 3.2 laser speckle image acquisition and image texture analysis

For the image acquisition, two groups of plant leaves have been selected. First group includes healthy leaf (Figure 1) and the second group includes Infected leaves by Shot hole Disease whose cellular or sub-cellular features are possibly modified. All laser speckle images as seen in figure 2 are taken by a high resolution camera at 3840x2880 pixel resolution. Diseased and healthy leaf tissues images of  $\lambda=6.5 \mu\text{m}$  laser Speckle images are sampled at 200x200 pixel (each refers to  $0.56\text{mm}^2$  area) with an image resolution of  $2.8 \mu\text{m}$  /pixel. The pattern differences in Figure 2 between the healthy and diseased image samples are invisible to naked eye. As is seen in figure 1b, Laser speckle imaging setup configuration consists of the camera and a laser source by which an image of cellular tissue is acquired. The laser wavelength  $\lambda= 0.65 \mu\text{m}$  is shorter than individual cell size ( $\sim 60\mu\text{m}$ ) or sub-cellular components size (e.g. cell nucleus) So that the laser can interact and back scatter by conveying the characteristic pattern of cellular components to the speckle image. The surface normal makes  $2^\circ$  angles with laser beam and camera viewing axis. The Figure 3 also indicates that the diseased and healthy leaf tissues images taken with a microscope magnification can not be visible to naked eye under normal light illumination as well as their laser speckle image equivalences.

The texture analysis is applied on each laser speckle image sample of the leaves classes (diseased/healthy) using 9 texture measures [5]. Texture image sample size are selected as 3x3 pixel windows for Area A, and 200x200 pixel windows for Area B as shown in Figure 1a. It was stated that [7] large window size generates large edge effect at the class edge but generate a texture measure with higher stability than smaller window.

### 3.3 Bayesian networks

Bayesian networks are well established classification method whose background information is available publicly in various sources. Bayesian networks (BN) are known in the literature as ‘directed acyclic graphs’ which perform knowledge representation and reasoning even under uncertainty. They are also called directed Markov fields, belief networks or causal probabilistic networks [9][10]. Its operational principles may be described by its generic Equation 6

$$P(X) = \prod_i P(X_i | pa(X_i)) \quad (6)$$

where :  $P(X)$  is the joint probability distribution which is the product of all conditional probabilities.  $pa(X_i)$  is the parent set of  $X_i$  (e.g. class node to decide normal/micro-collapse product) For the experiments the BN utility called PowerPredictor™ is used. The utility is used for automated network construction which accepts the continuous variables and uses Markov conditions to obtain a collection of CI statements from the network [14]. All valid CI relations can also be extracted from the topology of the network. The algorithm examines information of two related variables from a data set and decides if two variables are dependent. It also examines how close the relationship is between those variables. This information is called conditional mutual information of two variables  $X_i, X_j$  which may be denoted as:

$$I(X_i, X_j | C) = \sum_{x_i, x_j, c} P(x_i, x_j, c) \log \frac{P(x_i, x_j | c)}{P(x_i | c)P(x_j | c)} \quad (7)$$

In Equation 7, C is a set of nodes and c is a vector (one instantiation of variables in C). If  $I(X_i, X_j | C)$  is smaller than a certain threshold t, then we can say  $X_i$  and  $X_j$  are conditionally independent. This criteria is the basis of an automated network construction with the links between the network variables (nodes) as shown in Figure

In the experiments, ones the textural data set of laser speckle samplings is established, the well established classification method called Bayesian networks is used to distinguish between the diseased and healthy plant tissue whose micro scale changes are not visible to normal eye.

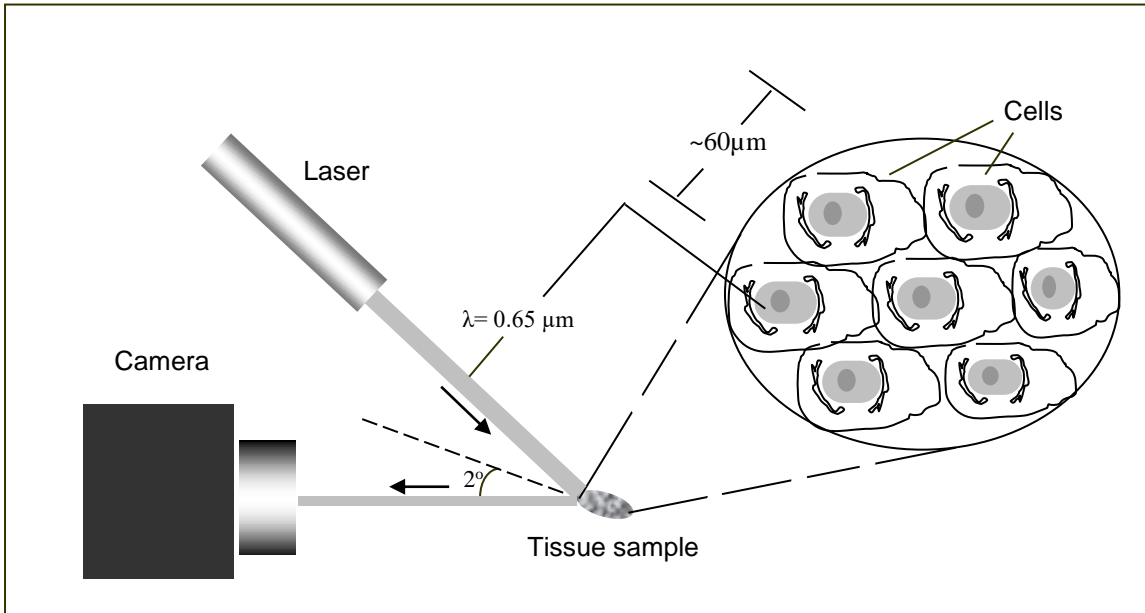


Figure 1b. Laser speckle imaging setup configuration by which an image of cellular tissue is acquired. The laser wavelength  $\lambda = 0.65 \mu\text{m}$  is shorter than individual cell size ( $\sim 60 \mu\text{m}$ ) or sub-cellular components size (e.g. nucleus) so that the laser can interact and back scatter by conveying the characteristic pattern of cellular components to the speckle image. The surface normal makes  $2^\circ$  angles with laser beam and camera viewing axis.



Figure 1. The healthy leaf (on the right) and Infected leaves by Shot hole Disease (on the left) whose cellular or sub-cellular features are modified.

### 3.4 Shot hole disease

Shot hole disease (also called *Coryneum blight*) is a serious fungal disease which effect plant leaves [13] generating large size holes as seen in Figure 1. The pathogen called *Wilsonomyces carpophilos* causes the disease which ends up with falling of the leaves. The higher the temperature the more quickly the disease is infected [14] The experimental observations have shown that at 25° environmental temperature the infection takes only 6 hours. The Fungal pathogen of Shot hole disease can persist several years in the infected plants. Within this work the experimental tests have proven that fungal pathogen population effect the leave tissue in homogenous form of cellular network, generating a texture effect which can only be measurable by specific textural analyses [5].

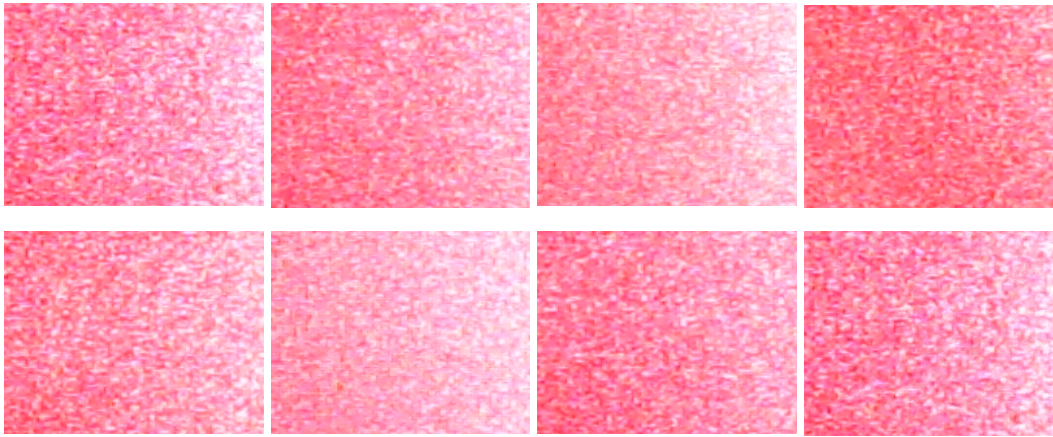


Figure 2. Diseased (top) and healthy (bottom) leaf tissues images of  $\lambda=6.5 \mu\text{m}$  laser Speckle sampling at 200x200 pixel ( $0.56\text{mm}^2$ ) with an image resolution of  $2.8 \mu\text{m}$  /pixel. The pattern differences between the top and bottom rows are invisible to naked eye.

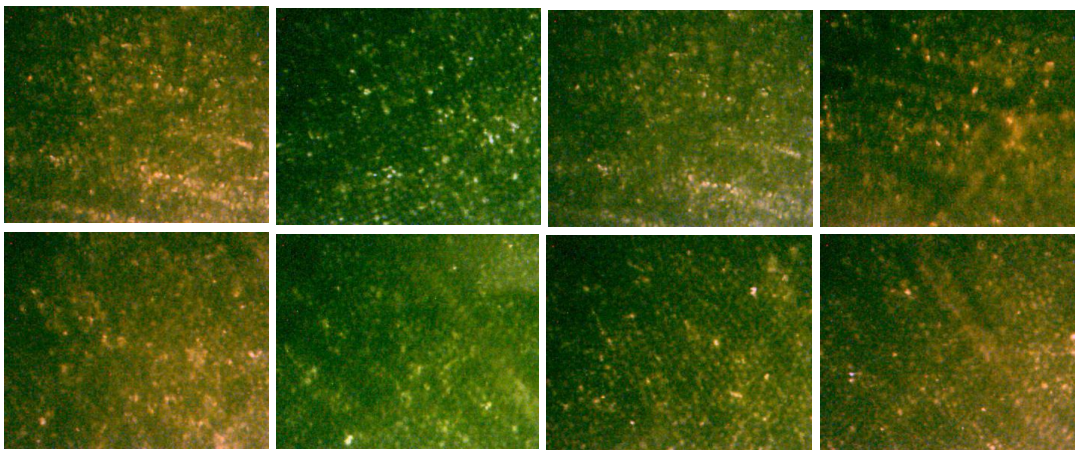


Figure 3. Diseased (top) and healthy (bottom) leaf tissues images with a microscope magnification (150x). As is seen the characteristic differences between diseased and healthy tissues can not be visible to eye under normal light illumination. .

## 4 Results and discussion

### 4.1 Experimental data set

The data set consists of 40 cases which correspond to leaf samplings taken from almost equal classes of healthy and diseased leaf populations. The attributes of data set belong to 9 texture measures whose pixel based statistics are already explained in Figure 1a. The reduced form of  $40 \times 10$  data set is shown in Table 1. The first group of texture measures (index1) refer to interior laser speckle band region which is just around the edge of laser bright spot area (marked as A), and the second group refers to exterior laser speckle band region (marked as B) as shown in Figure1a. The laser

speckle image data sampling is selected with an optimum pixel window as each window has to cover enough texture primitives for the pixel based textural statistics. Whereas the extremely larger pixel windows increase the computational cost unnecessarily. The sampling has also to be done to justify homogeneity of the texture windows which is inevitable for an accurate texture analysis [3]

Table I. Laser speckle image texture values of the leaf samplings. The first group of texture measures (index1) refer to interior laser speckle band region, and the second group refers to exterior laser speckle band region as shown in Figure1a. Classes “h” and “d” refer to healthy and diseased plants respectively. (here 40x10 data set is reduced for the display purpose)

| sample No. | russ1 | levine1 | sigm1 | skew1 | russ2 | levine2 | sigm2 | skew2 | stdev | Class |
|------------|-------|---------|-------|-------|-------|---------|-------|-------|-------|-------|
| 1          | 421   | 111     | 10.54 | 1.78  | 91    | 169     | 13    | -1.43 | 30.73 | h     |
| 2          | 524   | 190     | 13.78 | -0.2  | 318   | 258     | 16.06 | -2.65 | 32.8  | h     |
| 3          | 121   | 11      | 3.32  | 3.06  | 22    | 13      | 3.61  | 0.27  | 16.93 | h     |
| 4          | 219   | 26      | 5.1   | 2.24  | 28    | 38      | 6.16  | -0.02 | 20.58 | h     |
| 5          | 75    | 13      | 3.61  | 1.51  | 80    | 23      | 4.8   | 0.37  | 10.08 | h     |
| 6          | 281   | 63      | 7.94  | 0.97  | 83    | 101     | 10.05 | -0.82 | 20.96 | h     |
| .          | 428   | 753     | 27.44 | -1.52 | 304   | 862     | 29.36 | -2.05 | 40.57 | d     |
| .          | 209   | 48      | 6.93  | 0.63  | 62    | 75      | 8.66  | -1.09 | 28.64 | d     |
| .          | 177   | 25      | 5     | 2.74  | 16    | 37      | 6.08  | 0.37  | 23.29 | d     |
| .          | 163   | 19      | 4.36  | 2.76  | 44    | 26      | 5.1   | 0.42  | 20.54 | d     |
| 40         | 163   | 25      | 5     | 2.34  | 72    | 37      | 6.08  | 0.28  | 22.66 | d     |

By the proposed method called Intelligent laser speckle classification in which the appropriate imaging instruments (high resolution CCD camera and low level (1mW) red laser source are used as well as 9 texture measures shown in Figure1a, it is possible to distinguish between the diseased and healthy leaf tissue groups by use of Bayesian classifier PowerPredictor™ (Figure 4) with 87% accuracy. The test results strengthen the idea that the laser beam at  $\lambda=6.5$  micron wavelength can interact with relatively larger cellular or sub-cellular features such as the possible changes in cell membrane, cell nucleus or even nucleus content, and also unveil the changes between the two group of tissues like before and after chemical treatment or diseased and healthy situations.

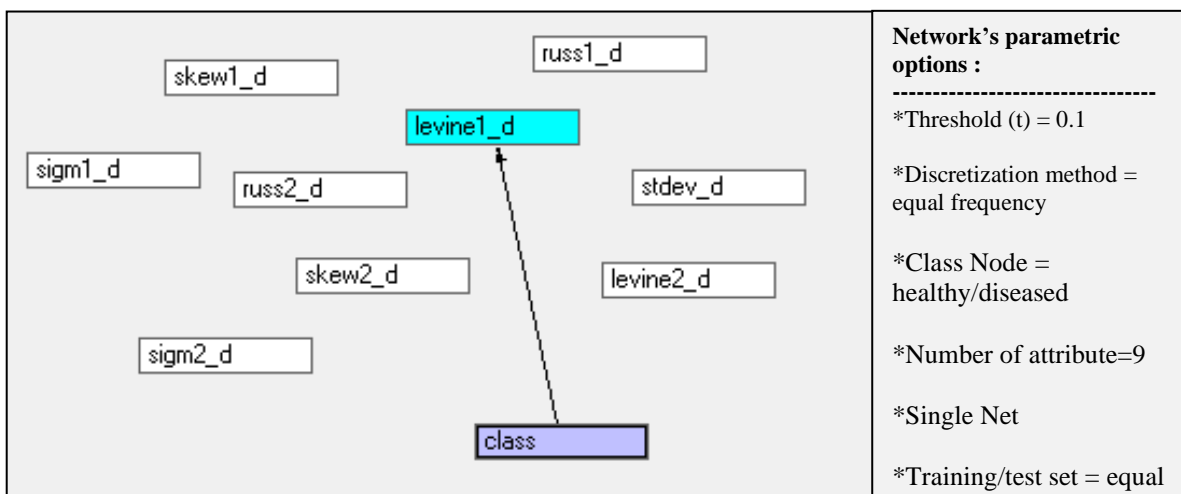


Figure 4. Attributes network build after BN training by whom 87% Classification accuracy is obtained to distinguish between the modified and normal sub-cellular contents of two classes. The same attributes are also exhibited in Table 1.

As is seen in BN network (Figure 4) the cellular or sub-cellular changes before and after the side effect of Shot hole disease could be classified through the texture measure Levine1 whose image sampling scan is achieved by (3x3) pixel window. The rest of texture measures are not linked since they would make less or equal contribution to the classification results. In the Bayesian network setup, the optimum system parameters are selected for the best output

such as; node connection *threshold* ( $t$ ) = 0.1 is selected to include highest number of attributes into the network (as described in Equation 7), The discretization method *Equal frequency* is also selected to obtain maximum classification accuracy with the available data structure. We have to note that, the nodes those are not connected are not excluded from the classification process but their inclusion to the network would not increase the classification accuracy.

## Conclusion

By use of Intelligent laser speckle classification technique supported by Bayesian Networks (PowerPredictor™) a classification result with 87% accuracy has been obtained to distinguish between the healthy and diseased plant cells in association with laser speckle effect. The test results have proven the theory that the laser beam at  $\lambda=6.5$  micron wavelength can interact with plant's cellular or sub-cellular features such as the cell membrane, cell nucleus or nucleus content. The method is also promising to unveil the subtle changes between the two group of tissues like before and after a chemical treatment, diseased or healthy conditions, etc. whatever factor effective at cellular scale. The work would be assumed as an initial stage of further improvement for the observations of human cellular changes (e.g. blood cells, skin or organs tissue cells) as human cell size is still smaller than the red laser wavelength. In addition to the size factor, red laser at  $\lambda=6.5$  micron is also optimal light for human's red blood cell reflection [15]. The proposed technique would be utilized for development of more accurate methods such as better drug delivery assessments as the drug taken by human body reaches to cells in a certain period and such model would be exploited to distinguish between before and after drug effects on the cellular structure and characteristics. The other application area would be the systemic disease inspection via skin analysis as the systemic diseases (e.g. diabetes, hearth disease, kidney disease, etc.) early signs can be exhibited by the skin cell content like insulin deposit for diabetes.

## References

- [1] A. B Orun<sup>1</sup>, E. Goodyer<sup>1</sup>, H. Seker<sup>1</sup>, G. Smith<sup>2</sup>, V. Uslan<sup>1</sup> and D. Chauhan., Optimized parametric skin modelling for diagnosis of skin abnormalities by combining light back-scatter and laser speckle imaging. *Skin Research and Technology* 2014; 0: 1–13.
- [2] Orun AB, Alkis A. Material identification by surface reflection analysis in combination with bundle adjustment technique. *Pattern Recognition Letters* 2003; 24: 1589–1598.
- [3] A. B. Orun, H. Seker, V. Uslan, E. Goodyer and G. Smith., Texture-based characterization of sub-skin features by specified laser speckle effects at  $\lambda = 650$  nm region for more accurate parametric 'skin age' modelling. *International Journal of Cosmetic Science*, 2016, 1–7
- [4] Rabal, H., J., and R.A. Braga. *Dynamic laser speckle and applications*. CRT Press. Taylor & Francis, 2009.
- [5] Phillips D. Image processing in C, part 15: basic texture operations. *C/C++ Users J* 1995; 13: 55–68.
- [6] Orun AB, Aydin N. Variable optimisation of medical image data by the learning Bayesian Network reasoning, 32nd Annual International Conference of the IEEE Engineering in Medicine and Biology Society (EMBC'10), Buenos Aires, Argentina, 1–4 September 2010.
- [7] Christopher, J., S, Warner TA. Scale and texture in digital image classification. *Photogrammetry Eng. And Remote Sensing* 2002; 68: 51–63
- [8] Orun, A.B and Alkis, A. "Material identification by surface reflection analysis in Combination with Bundle Adjustment Technique", *Pattern Recognition Letters*, Elsevier Science, Vol. 24, No. 9-10, June 2003.
- [9] Jensen F. *An introduction to Bayesian networks*. New York: Springer; 1998
- [10] Cheng J, Bell D, Liu W. Learning Bayesian networks from data: an efficient approach based on information theory. 2002. <http://www.cs.ualberta.ca/~jcheng/lab.htm>
- [11] Orun, A.B and G.Smith (2017) Micro-structural analysis of tablet surface layers by intelligent laser speckle classification (ILSC) technique: An application in the study of both surface defects and subsurface granule structures. *Journal of Pharmaceutical Innovation*.Vol.12, No.4.

[12] Mahe, G., Rousseau, P., Durand, S., Bricq, S., Leftheriotis, G. and Abraham, P. Laser speckle contrast imaging accurately measures blood flow over moving skin surface. *Microvasc. Res.* 81, 183–188 (2011).

[13] Bubici, G. M. D'Amico and M.Cirulli. Field reaction of plum cultivars to the shot-hole disease in southern Italy. *Crop Protection*, Vol.29 (12), pp. 1396-1400.

[14] [http:// en.wikipedia.org/wiki/Shot\\_hole\\_disease](http://en.wikipedia.org/wiki/Shot_hole_disease)

[15] Butkus, B.D. Blood-flow imaging adapted for endoscopy. *Biophotonics, Int* 2003; 10: 17–20.